Geochemical Perspectives Letters

A global imbalance in potassium and barium river export: the result of biological uptake?

Q. Charbonnier[1,2*], J. Bouchez[1], J. Gaillardet[1,3], E. Gayer[1], S. Porder[4]

OPEN ACCESS

https://doi.org/10.7185/geochemlet.2214

Abstract

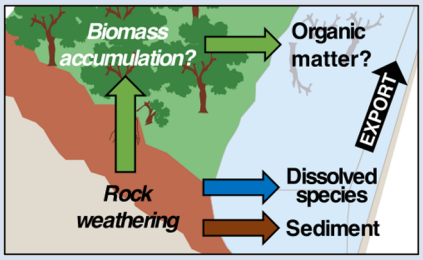

The role of biological cycling on the chemistry of rivers remains poorly understood. In an attempt to close this knowledge gap, here we examine the difference between the elemental supply to catchments through rock degradation and the corresponding elemental riverine export, for two non-nutrient elements lithium (Li) and sodium (Na) and two nutrients-like elements potassium (K) and barium (Ba), in 20 of the largest world river catchments. Overall, the riverine export of K and Ba are lower than their estimated release by catchment scale rock degradation, while the two fluxes match for Li and Na. Barium isotope constraints lending support to this observation, we take this difference between these two element groups as a suggestion of the influence of biological uptake of rock-derived nutrients on river chemistry. Nevertheless, the magnitude of riverine K depletion cannot be reconciled with a pervasive growth of the biota on continents, nor with an "occult" export of organic material that would go unnoticed by common sampling protocols. One plausible explanation for this conundrum could lie in the complex partitioning of elements amongst soil, biota, and dead organic matter. As a consequence, our study emphasises the need for further work aiming at deciphering the cycle of rock-derived nutrients in the Critical Zone.

Received 16 November 2021 | Accepted 29 March 2022 | Published 5 May 2022

Introduction

The Earth surface hosts a suite of complex interactions between the lithosphere, the hydrosphere, the atmosphere, and the biosphere which all occur in the "Critical Zone" (CZ) between un-weathered rock and the atmosphere (Riebe *et al.*, 2017). Chemical weathering within the CZ regulates atmospheric CO_2 over million year timescales, influences soil formation, and releases rock-derived nutrients to ecosystems, thereby profoundly influencing life on Earth (Gaillardet *et al.*, 2018).

As the CZ cannot be sampled in its totality, river chemistry is an integral tool for large scale studies of the CZ processes. River loads of base cations (Na^+, K^+, Mg^{2+}, and Ca^{2+}) and dissolved silica (SiO_2) are commonly used to derive catchment scale weathering fluxes and associated CO_2 consumption (Bouchez and Gaillardet, 2014). This approach assumes some balance between the production of major solutes by rock weathering and their riverine export. However, this assumption is falsified if processes exist in the CZ that transiently store base cations. In particular, the biological uptake of the major rock-derived nutrients Ca, Mg, K, and Si is almost always assumed to be in balance with their release during organic matter degradation in soils (Viers *et al.*, 2014). Were this assumption violated, river chemistry would not faithfully record chemical weathering processes and rates. An apparent deficit of rock-derived nutrients in the river load, together with shifts in their isotope signatures, has been reported for a range of bio-utilised elements such as K, Mg, Ca, P and Ba in streams (von Blanckenburg *et al.*, 2021) as well as in the Amazon (Charbonnier *et al.*, 2020), suggestive of imbalance in the export of rock-derived nutrients. Such deficit might be due to changes in the size of the biological reservoir with time beyond the typical observational time scale of a few years; or might occur if the transport of unsampled river particulate organic matter constitutes a significant pathway of rock-derived nutrient export from the catchment.

Here we show that data from the largest world rivers provide evidence for a global imbalance in the river export of cations, and examine the role potentially played by the biota as an "embezzler" of nutrient river fluxes (Fig. 1). We achieve this goal through the comparison of estimates of rock-derived nutrients supply to the CZ though rock weathering – along with their isotopes – against their actual riverine export.

A Global Imbalance in Rock-Derived Nutrient Riverine Export from the Critical Zone

We quantify the catchment scale budgets between rock degradation by chemical weathering and subsequent riverine export for some of the world largest rivers, for a series of elements: lithium (Li), sodium (Na), potassium (K), barium (Ba). Large rivers

1. Université de Paris, Institut de Physique du Globe de Paris, CNRS, F-75005 Paris, France
2. Institute of Geochemistry and Petrology, Department of Earth Sciences, ETH Zurich, Clausiusstraße 25, 8092 Zurich, Switzerland
3. Institut Universitaire de France, Paris, France
4. Institute at Brown for Environment and Society, Brown University, Providence, Rhode Island 02912 USA
* Corresponding author (email: quentin.charbonnier@erdw.ethz.ch)

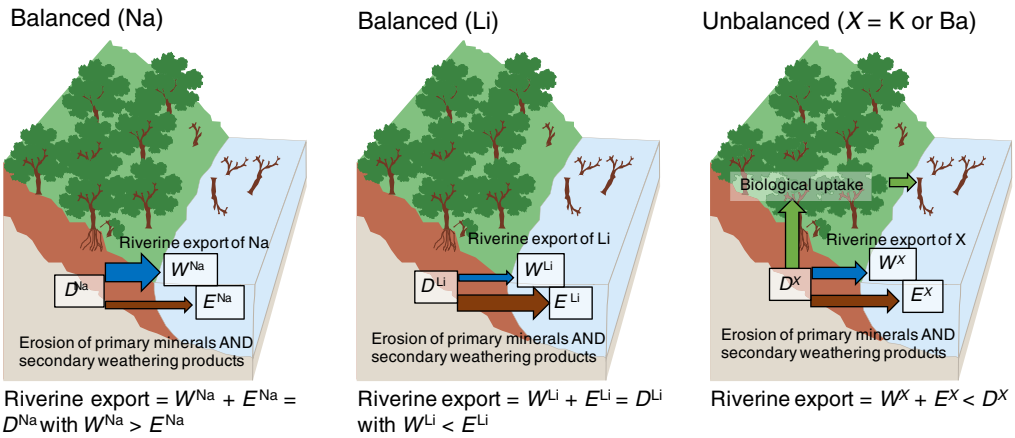

Figure 1 Conceptual sketch of the catchment scale mass budgets, for X = Na, Li (non-nutrients) and for nutrient/nutrient-like elements (X = K and Ba). This approach aims to quantify the catchment scale (im)balance between the supply of a rock-derived nutrient X through rock degradation (D^X) and the summed dissolved and solid riverine export (W^X and E^X, respectively). The difference in the "solubility" translates into a difference in the size of the W^X and E^X arrows.

draining significant portions of the continents offer unique access to first order, global information on the cycle of elements. The set of large rivers considered here encompasses various geological, geomorphological, and climatic contexts. Detail on sample locations and analytical methods is provided in the Supplementary Information, together with a full derivation of the mass balance equations used to quantify the river mass budget.

Briefly, in this approach inspired from previous work such as Gaillardet *et al.* (1999), we establish the equation: bedrock = dissolved load + particulate load, for some silicate-derived soluble elements (*i.e.* partitioned between the dissolved and residual particulate phases of weathering) such as here lithium, sodium, potassium and barium, as well as for insoluble elements (such as aluminium, samarium and thorium) that are only transported in the particulate form (Fig. 1). Graphically, data for different elements and rivers can then be plotted in a diagram representing the fraction of the soluble element X transported in the dissolved load, against the relative depletion factor of this soluble element in the particulate load (compared to bedrock), as in Figure 2. A balanced river mass budget is manifested as data points lying on the down sloping diagonal in Figure 2, whereas depletion of X in the total river export (be it a deficit in the river dissolved or solid load) translates into data points below this diagonal. Critically, partitioning of X between the dissolved and solid river exports does not have any influence on the results of the river

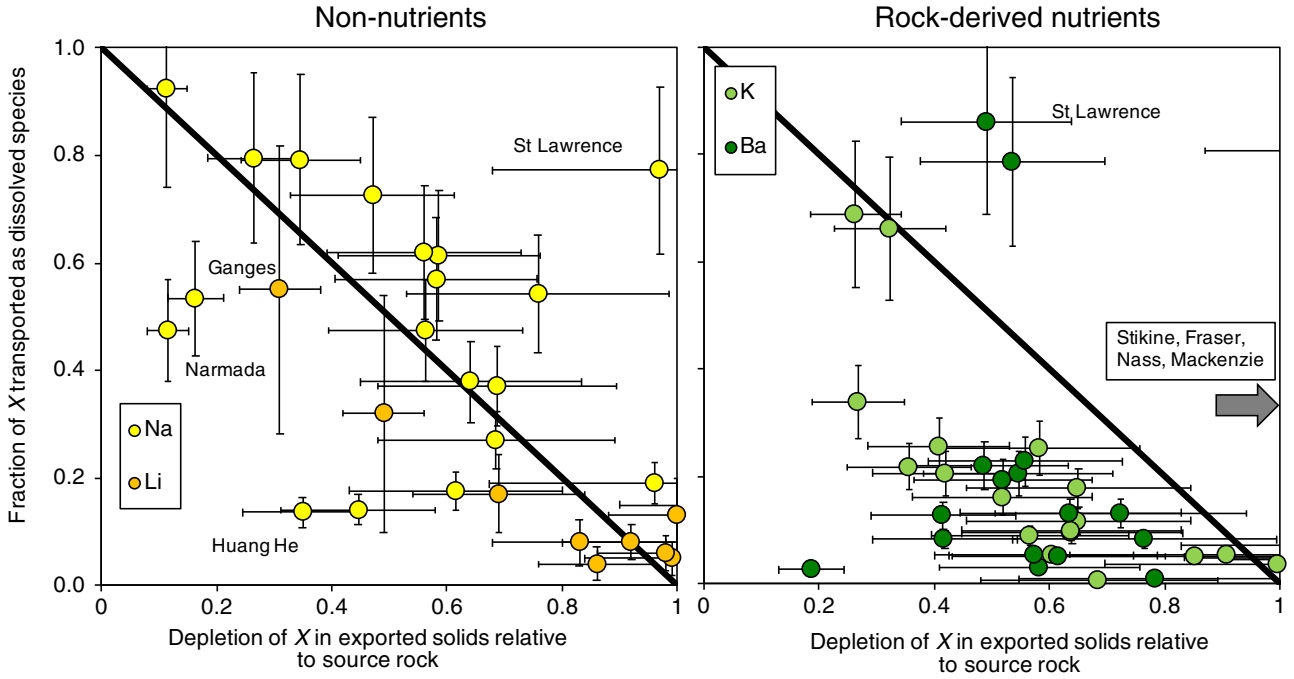

Figure 2 Comparison between the relative dissolved export of an element X and its depletion in river solids compared to source rock for X = Na, Li, K, and Ba for some of the world largest rivers. A catchment scale balance between river export and supply by rock degradation is represented by the diagonal line. The root mean square deviation from the trend of a balanced budget (diagonal line) is much higher for Ba and K (0.51 and 0.35, respectively) than for Na and Li (0.14 and 0.11, respectively). Detail about calculations is provided in the Supplementary Information.

mass budget, as it does not move data points away from or closer to the diagonal. Rather, this analysis is only sensitive to whether the overall elemental riverine export reflects the abundance of this element in the rock weathered.

In the world's largest rivers, for the two non-nutrient elements sodium (major element, Na) and lithium (trace element, Li), the supply to the CZ by rock degradation is balanced by the combined dissolved and solid riverine export (Figs. 2, 3). Such agreement was already noticed based on Li isotopes by Dellinger *et al.* (2015). Such balance is remarkable as the formation of river solids and solutes in soils by chemical weathering operate over different timescales, implying that at any time varying soil formation and erosion should lead to significant imbalance in river mass budgets. In other words, this observation suggests that the formation of secondary weathering phases in the CZ, such as clays or (hydr)oxides in soils, is balanced by their export as river solids, and that consequently no significant net accumulation of a Li-bearing secondary phase within the global CZ is occurring.

Conversely, the major rock-derived nutrient potassium (K; group 2 in the classification of Marschner *et al.*, 1996) and the minor, nutrient-like element barium (Ba; Bullen and Chadwick, 2016) show a widespread imbalance between supply to the CZ and riverine export fluxes by rivers (Fig. 2), consistent with previous studies on headwater catchments (von Blanckenburg *et al.*, 2021) and in the Amazon (Charbonnier *et al.*, 2020). Collectively, these results suggest that Ba and K sourced from silicate weathering are fractionated between a "residual" reservoir in the CZ and the total riverine export.

Accumulation of secondary phases of weathering within the CZ could explain this deficit. However, in such a scenario our data would reflect the formation and accumulation of specific, Ba- and K-hosting phases not exported by rivers, at least not in the same way as Na and Li. These Ba- and K-bearing phases could be of inorganic nature. In fact, the K and Ba river mass budget equations used here are relative to the insoluble element thorium (Th), meaning that the observed imbalance suggests the formation of high Ba/Th and K/Th reservoirs within the CZ, whereas the river export is lower in Ba/Th and K/Th compared to source silicate rocks. Given the insoluble and non-nutrient nature of Th, such enriched Ba and K components can hardly derive from the scavenging into classical secondary

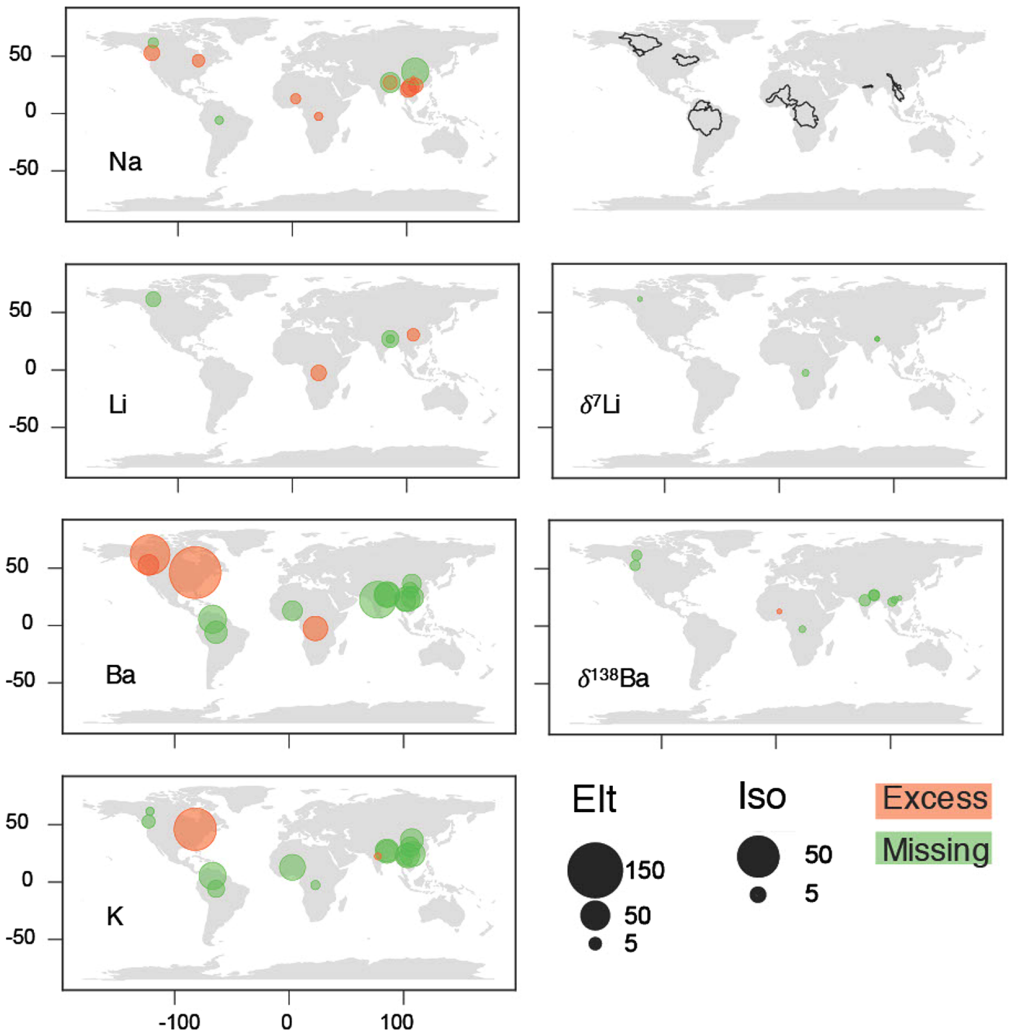

Figure 3 Quantification of catchment scale elemental and isotope (im)balance for the world largest rivers using river mass budgets. The upper right map indicates the studied river catchments. Elemental imbalance ("Elt") is expressed in percentage, and the isotope imbalance ("Iso") is expressed as the isotope difference quantified in Equation S-8. Due to the mass difference between Ba and Li, the magnitude of isotope fractionation is much larger for Li than for Ba, resulting in larger numbers for the isotope imbalance. To make the numbers for both isotope systems comparable, we multiply each of the "raw" numbers for the isotope imbalance (as quantified by Eq. S-8) by the ratio between the mass of the element (*e.g.*, 137.32 for Ba) and the difference of mass of the two isotopes used (*e.g.*, 138 – 134 = 4 for Ba).

soil phases. Even though iron oxides can be characterised by higher Ba/Th ratios than silicate minerals (Gong *et al.*, 2019), such phases should be exported from the CZ together with other secondary phases of weathering. Further, K does not show such enrichment in iron oxides (Gong *et al.*, 2019), showing that the positive relationship between the magnitudes of Ba and K imbalance (Fig. S-4) cannot derive from a global retention of iron oxides in soils. This analysis argues for a role of organic phases in the Critical Zone in producing the observed global K and Ba imbalance.

Furthermore, the Ba river export by most large rivers is characterised by an isotope signature heavier than that of the Ba input to the CZ by rock degradation (see Supplementary Information; Fig. 3). This either means that heavier-than-thought Ba is released to the CZ during rock degradation, or that a Ba component enriched in the light isotope is missing. Regarding the first possibility, recent work suggests that the weathering of black shales delivers heavy Ba isotope signatures (Charbonnier *et al.*, 2022). Nevertheless, such a heavy Ba flux is associated with an elemental excess of Ba (Charbonnier *et al.*, 2022), which is observed only for the Mackenzie Basin in the present global dataset. Furthermore, no relationships between dissolved Ba isotopes and sulfate content or osmium isotopes (two tracers of black shale weathering) emerge (not shown). Therefore, an isotopically light reservoir of Ba must exist in the global CZ. As suggested above, this isotopically light Ba reservoir could reflect the formation of secondary weathering products and their retention in soils (Gong *et al.*, 2019), or biological uptake (Bullen and Chadwick, 2016).

Barium adsorption onto river sediments, although able to account for variations in dissolved Ba isotopes (Bridgestock *et al.*, 2021), cannot influence the results of river mass budgets, which sum together the signatures of the dissolved and solid river loads leading to an isotope neutral effect for the processes partitioning the elements between the different river phases. Finally, formation and retention of secondary weathering products in soils should result in a strong Li isotope imbalance, as the light isotope of Li is preferentially incorporated in these phases (Pogge von Strandmann *et al.*, 2012). As this is contradictory to our observations (Fig. 3), we are left with biological uptake as the only explanation for the relatively heavy Ba isotope composition in our global river dataset.

Testing for the Role of Biological Uptake in Deleting the River K and Ba Exports

Taken at face value, the depleted river export of rock-derived nutrients might reflect their locking within biological materials through two categories of phenomena. First, (1) the corresponding biological material could be exported from catchments as particulate organic carbon that is not adequately sampled. For example, Abbe and Montgomery (2003) have shown that significant river transport of woody debris would not be properly accounted for by traditional methods used for sampling large rivers. Another possibility for such "hidden" export of particulate organic matter is tree logging by human activities. Alternatively, (2) accumulation of biological material within the catchment as above or underground biomass or as litter would also result in an imbalance, at least over the timescale over which the data used for the river mass budget are collected. Below, we show how the results of our investigations are difficult to reconcile with these scenarios.

First of all, basins characterised by the strongest negative imbalance in the river mass budgets of rock-derived nutrients are not characterised by the strongest logging activities (see Supplementary Information). Therefore to test for scenario (1) above, that is one of a "ungauged organic flux", we estimate the amount of river particulate organic carbon (C) that would be needed to account for the observed imbalance in K (Fig. S-5) by using a typical K/C mass ratio for plant material of 0.0012 (Charbonnier *et al.*, 2020). For a given catchment, the inferred missing flux of river particulate organic C is more than two orders of magnitude higher than the river export of particulate organic carbon estimated by Galy *et al.* (2015) (Fig. S-5). It seems unrealistic that 99 % of the biogenic particulate organic carbon is exported through poorly- or non-sampled episodic and/or coarse vegetation debris in large river systems for this K/C ratio (a ratio the validity of which will be further discussed).

The likelihood of organic matter accumulation within catchments as an explanation for the global imbalance in catchment scale mass budgets (a "growing organic pool" scenario, labelled as (2) above) can first be appraised using a back-of-the-envelope calculation. Using typical K concentrations in rocks and plants and estimates of organic matter stocks in biomass and soils (see Supplementary Information), we calculate that an annual 0.1–0.2 % increase in the biomass can explain the observed imbalance in K catchment scale mass budgets. Although the time scale over which the observed catchment scale imbalance is established remains elusive, we note that if such an increase in biomass or organic matter were sustained over 30 yr – a period over which we believe constraints on the global land carbon pools are reasonable – this would result in an overall biomass growth by 3.5–8.0 %, which has not been reported (Friedlingstein *et al.*, 2020).

Overall, the results of the first order calculations presented above challenge the biological uptake role in deleting the global river exports of K and Ba. However, we also note that some degree of decoupling might exist between biological uptake and riverine export of rock-derived nutrients. In particular, biological activity is known to exert an indirect control on the distribution of rock-derived nutrients and their isotopes amongst the different CZ compartments (Bullen and Chadwick, 2016). For example, the top layer of soils accumulates a sizeable reservoir of nutrients that are readily accessible for the biota, a feature known as "bio-lifting" (Jobbágy and Jackson, 2004). If these topsoil horizons were disproportionately contributing to the global river particulate carbon export, such enrichment leading to elevated nutrient-to-carbon ratios in exported organic matter would require revision of the K/C ratio used above, possibly to a level where the scenarios explored above would become plausible. Clearly, further work is needed to pinpoint how life might (a) transiently divert rock-derived nutrients released by rock weathering from river export, and (b) partition rock-derived nutrients amongst the CZ compartments.

Implication for the Study of Critical Zone Processes from River Chemistry

The global balance of riverine Li and Na and the global imbalance of riverine K and Ba, supported by isotopic observations, raises the possibility that nutrient-like elements are "diverted" from the riverine export, and may constitute a tangible influence of biological uptake on riverine export of rock-derived nutrients.

Nonetheless, comparison between the depleted flux of riverine K and Ba cannot be reconciled with reasonable figures for globally growing biomass, or for unsampled biogenic river components, indicating that the exact distribution of rock-derived nutrients amongst the various CZ compartments constitutes a critical knowledge gap. Overall, contrasting patterns between riverine exports of nutrient and non-nutrient elements

suggest that major river cations are likely "less conservative" than previously thought. As a consequence, the way geochemical processes are deduced from river chemistry might warrant reconsideration.

Acknowledgements

The authors thank Pascale Louvat, Thibaud Sontag, Jessica Dallas, and Pierre Burckel for analytical support. Geochemical analysis presented in this study were enabled by the IPGP multidisciplinary programme PARI, by the Region Île-de-France SESAME grant no. 12015908, and by the "Émergences" grant awarded by the City of Paris to Julien Bouchez. Eric H. Oelkers is thanked for editorial handling of the paper. Three anonymous reviewers are thanked for their constructive comments that improved the paper.

Editor: Eric H. Oelkers

Additional Information

Supplementary Information accompanies this letter at https://doi.org/10.7185/geochemlet.2214.

Cite this letter as: Charbonnier, Q., Bouchez, J., Gaillardet, J., Gayer, E., Porder, S. (2022) A global imbalance in potassium and barium river export: the result of biological uptake? *Geochem. Persp. Let.* 21, 32–36. https://doi.org/10.7185/geochemlet.2214

References

Abbe, T.B., Montgomery, D.R. (2003) Patterns and processes of wood debris accumulation in the Queets river basin, Washington. *Geomorphology* 51, 81–107. https://doi.org/10.1016/S0169-555X(02)00326-4

Bouchez, J., Gaillardet, J. (2014) How accurate are rivers as gauges of chemical denudation of the Earth surface? *Geology* 42, 171–174. https://doi.org/10.1130/G34934.1

Bridgestock, L., Nathan, J., Paver, R., Hsieh, Y.-T., Porcelli, D., Tanzil, J., Holdship, P., Carrasco, G., Annammala, K.V., Swarzenski, P.W., Henderson, G.M. (2021) Estuarine processes modify the isotope composition of dissolved riverine barium fluxes to the ocean. *Chemical Geology* 579, 120340. https://doi.org/10.1016/j.chemgeo.2021.120340

Bullen, T., Chadwick, O. (2016) Ca, Sr and Ba stable isotopes reveal the fate of soil nutrients along a tropical climosequence in Hawaii. *Chemical Geology* 422, 25–45. https://doi.org/10.1016/j.chemgeo.2015.12.008

Charbonnier, Q., Bouchez, J., Gaillardet, J., Gayer, É. (2020) Barium stable isotopes as a fingerprint of biological cycling in the Amazon River basin. *Biogeosciences* 17, 5989–6015. https://doi.org/10.5194/bg-17-5989-2020

Charbonnier, Q., Bouchez, J., Gaillardet, J., Calmels, D., Dellinger, M. (2022) The influence of black shale weathering on riverine barium isotopes. *Chemical Geology* 594, 120741. https://doi.org/10.1016/j.chemgeo.2022.120741

Friedlingstein, P., O'Sullivan, M., Jones, M.W., Andrew, R.M., Hauck, J., *et al.* (2020) Global Carbon Budget 2020. *Earth System Science Data* 12, 3269–3340. https://doi.org/10.5194/essd-12-3269-2020

Dellinger, M., Bouchez, J., Gaillardet, J., Faure, L. (2015) Testing the Steady State Assumption for the Earth's Surface Denudation Using Li Isotopes in the Amazon Basin. *Procedia Earth and Planetary Science* 13, 162–168. https://doi.org/10.1016/j.proeps.2015.07.038

Gaillardet, J., Dupré, B., Allègre, C.J. (1999) Geochemistry of large river suspended sediments: silicate weathering or recycling tracer? *Geochimica et Cosmochimica Acta* 63, 4037–4051. https://doi.org/10.1016/S0016-7037(99)00307-5

Gaillardet, J., Braud, I., Hankard, F., Anquetin, S., Bour, O., *et al.* (2018) OZCAR: the French Network of Critical Zone Observatories. *Vadose Zone Journal* 17, 1–24. https://doi.org/10.2136/vzj2018.04.0067

Galy, V., Peucker-Ehrenbrink, B., Eglinton, T. (2015) Global carbon export from the terrestrial biosphere controlled by erosion. *Nature* 521, 204–207. https://doi.org/10.1038/nature14400

Gong, Y., Zeng, Z., Zhou, C., Nan, X., Yu, H., Lu, Y., Li, W., Gou, W., Cheng, W., Huang, F. (2019) Barium isotopic fractionation in latosol developed from strongly weathered basalt. *Science of The Total Environment* 687, 1295–1304. https://doi.org/10.1016/j.scitotenv.2019.05.427

Jobbágy, E.G., Jackson, R.B. (2004) The uplift of soil nutrients by plants: Biogeochemical consequences across scales. *Ecology* 85, 2380–2389. https://doi.org/10.1890/03-0245

Marschner, P. (1996) *Marschner' s Mineral Nutrition of Higher Plants*. Third Edition, Elsevier, Amsterdam. https://doi.org/10.1016/C2009-0-63043-9

Pogge von Strandmann, P.A.E., Oppergelt, S., Lai, Y.-J., Sigfússon, B., Gislason, S. R., Burton, K.W. (2012) Lithium, magnesium and silicon isotope behaviour accompanying weathering in a basaltic soil and pore water profile in Iceland. *Earth and Planetary Science Letters* 339–340, 11–23. https://doi.org/10.1016/j.epsl.2012.05.035

Riebe, C.S., Hahm, W.J., Brantley, S.L. (2017) Controls on deep critical zone architecture: a historical review and four testable hypotheses. *Earth Surface Processes and Landforms* 42, 128–156. https://doi.org/10.1002/esp.4052

Viers, J., Oliva, P., Dandurand, J.-L., Dupré, B., Gaillardet, J. (2014) 7.6 - Chemical Weathering Rates, CO_2 Consumption, and Control Parameters Deduced from the Chemical Composition of Rivers. In: Holland, H.D., Turekian, K.K. (Eds.) *Treatise on Geochemistry*. Second Edition, Elsevier, Amsterdam, 175–194. https://doi.org/10.1016/B978-0-08-095975-7.00506-4

von Blanckenburg, F., Schuessler, J.A., Bouchez, J., Frings, P.J., Uhlig, D., Oelze, M., Frick, D.A., Hewawasam, T., Dixon, J., Norton, K. (2021) Rock weathering and nutrient cycling along an erodosequence. *American Journal of Science* 321, 1111–1163. https://doi.org/10.2475/08.2021.01

Geochemical Perspectives Letters

A global imbalance in potassium and barium river export: the result of biological uptake?

Q. Charbonnier, J. Bouchez, J. Gaillardet, E. Gayer, S. Porder

Supplementary Information

The Supplementary Information includes:

1. Sample Set and Sampling Methodology

The sampling locations of the rivers analysed in this study are presented in Figure S-1. Most river samples come from the sample repository of Institut de Physique du Globe de Paris, and were collected over the 1990–2000 decades during various sampling campaigns (Gaillardet *et al.*, 1999a, 1999b; Lemarchand *et al.*, 2000; Tipper *et al.*, 2006, 2010). Time series from Arctic rivers and from the Congo Basin were collected by other research groups (Holmes *et al.*, 2012; Spencer *et al.*, 2012). Altogether, this dataset includes the Congo and Niger rivers in Africa, the Brahmaputra, Ganges, Hong He, Irrawaddy, Mekong, Narmada, Salween, and Tapti rivers in southeast Asia; the Changjiang, Huang He, and Xijiang rivers in China, the Amazon, Madeira, Solimões, Negro, and Orinoco rivers in South America; the Fraser, Kolyma, Lena, Mackenzie, Nass, Ob, St-Lawrence, Stikine, Yenisey, and Yukon rivers in the Arctic region; and the Seine in Europe. The cumulative water discharge represented by this

data set (letting aside the Solimões, Madeira, and Negro which are tributaries of the Amazon, already featured in the sample set) is around 36 % of the global water discharge to the ocean, and their cumulative surface represents 37 % of the continental surface draining to the oceans (Milliman and Farnsworth, 2011).

Classically, river water is filtered immediately after collection through 0.2-µm porosity cellulose acetate or poly-ether sulfone filters, using Teflon-coated, under-pressure filtration units. Filtered river water represents the dissolved load, while suspended sediments are retrieved from the filter, but note that in the present study as in many others, colloidal matter (that is, solids in suspension but with size <0.2 µm) is operationally considered to be part of the dissolved load. Because of their low hydrolysis constant, the four soluble elements considered here (Na, Li, K, Ba) are not likely to be strongly complexed to organic colloids nor present in significant amount in colloidal-sized clay particles. However, a significant fraction of the insoluble element loads used for normalization in the mass budget equations (section S-4) such as Th, can be present in this colloidal fraction, which can generate some bias for rivers rich in colloids, as discussed below.

Importantly for the topic addressed in the present study, because with the adopted sampling scheme in most large river studies, with a typical volume of a river water sample is in the range 0.5 to ~10 L, large organic debris (macrophytes, trunks) cannot be sampled, and their contribution to the river POC export is missed by this sampling scheme. However, fine organic material, being associated to minerals or transported as small organic debris, can be retrieved on filters (Galy *et al.*, 2008).

2. Analytical Methods

Both the elemental and isotope data for river dissolved and solid loads are reported in Table S-1.

2.1 Major and Trace Element Determinations

Major and trace element concentrations of river sediments were measured by ICP-AES and ICP-MS, respectively, at the SARM (Service d'Analyse des Roches et des Minéraux, INSU facility, Vandoeuvre-les-Nancy, France; analytical details available at http://helium.crpg.cnrs-nancy.fr/SARM). Major cation and anions of the dissolved load were

measured using ionic chromatography, while dissolved silica has been measured using UV-Vis spectrophotometry. Trace elements in the dissolved load were measured using ICP-MS, all at the High-Resolution Analytical Platform (PARI) of IPGP. Except for Ba abundance, all major element concentration data are from Lemarchand *et al.* (2000).

2.2 Isotope Measurements

For the present study, only barium (Ba) stable isotope ratios were analysed, as all other isotope measurements (lithium: Li) were already reported in previous studies (Dellinger *et al.*, 2014, 2015a, 2015b, 2017; Wang *et al.*, 2015; Henchiri *et al.*, 2016). The protocols for Ba separation and isotope measurements are described in Charbonnier *et al.* (2020). Briefly, a minimum of 200 ng Ba for each sample was separated from the sample matrix by ion chromatography (AG50W-X8 resin) using 2.5 N HCl to elute the matrix and 6 N HCl to elute Ba. For each sample, the separation procedure was performed two times to ensure a complete purification. The isotopic ratios were measured by MC-ICP-MS (Thermo Fisher Scientific, Neptune) at the PARI analytical platform of IPGP. Mass instrumental fractionation was corrected for using sample-standard bracketing. The interference of Xe on mass 134 was corrected for by on-peak zeroes. Barium isotopic ratios in the samples and standards were measured as:

$$\delta^{x}\mathrm{Ba} = \left(\frac{\left(\frac{^{x}\mathrm{Ba}}{^{134}\mathrm{Ba}}\right)_{\mathrm{sample}}}{\left(\frac{^{x}\mathrm{Ba}}{^{134}\mathrm{Ba}}\right)_{\mathrm{standard}}} \right) \times 1000 \qquad \text{Eq. S-1}$$

with x = 137 or 138. The standard used in this study was the NIST SRM 3104a. For the sake of consistency, data were converted to $\delta^{138/134}$Ba assuming that $\delta^{138/134}\mathrm{Ba} \approx 1.33 \times \delta^{137/134}\mathrm{Ba}$. Uncertainties on δ^{138}Ba are reported as 95 % confidence interval following a Student distribution, and are typically between 0.04 and 0.20 ‰. The long-term accuracy of the data was checked using the JB-2 (0.04 ± 0.16, 2 s.d., n = 7), Babe27 (−0.80 ± 0.15, 2 s.d., n = 7), BHVO-2 (−0.01 ± 0.15, 2 s.d., n = 8) and AGV-2 (0.05 ± 0.15, 2 s.d., n = 16) reference materials (Miyazaki *et al.*, 2014; van Zuilen *et al.*, 2016; Charbonnier *et al.*, 2018; Gou *et al.*, 2020).

3. Global Input of Barium to the Ocean

The isotope cycle of Ba has recently gained momentum due to its potential for reconstructing the strength of the ocean biological pump through geological timescales (Horner *et al.*, 2015; Bridgestock *et al.*, 2018, 2019), but the use of this proxy requires constraining the riverine input of Ba to the ocean. Below, because of the novelty of these Ba isotope data, we provide an analysis of the dissolved and solid riverine fluxes of Ba from the world largest rivers.

3.1 Abundance and Isotope Signature of Ba in the Global Solid Riverine Export

The Ba abundance in river suspended sediments shows significant variation from 138 mg/kg (Narmada) to 948 mg/kg (Stikine). The Ba/Th ratio of river sediment which, unlike Ba concentration, is not affected by dilution by Ba free-phases such as quartz, ranges from 15 to 263, and thus for some rivers differs significantly from the upper continental crust (UCC) value (Ba/Th ≈ 50; Taylor and McLennan, 1995; Rudnick and Gao, 2014). The δ^{138}Ba values of river suspended sediments (denoted $\delta^{138}Ba_{spm}$ in the following, 'spm' standing for "suspended particulate matter") vary between −0.14 and +0.34 ‰, whereas that of riverbed sediments (called $\delta^{138}Ba_{rbs}$ hereafter) range from −0.25 to +0.36 ‰ (Table S-1, Fig. S-2). River material $\delta^{138}Ba_{spm}$ values are thus significantly different from the Ba isotope composition the UCC (0.00 ± 0.04 ‰; Nan *et al.*, 2018). For any given river, $\delta^{138}Ba_{spm}$ and $\delta^{138}Ba_{rbs}$ are close to one another, suggesting a relative invariance of sediment Ba isotope composition despite grain size variations (Bouchez *et al.*, 2011), in contrast with results for other isotope systems (Dellinger *et al.*, 2014; Garçon *et al.*, 2014) but in agreement with observations made for Ba from river depth profiles in the Amazon Basin (Charbonnier *et al.*, 2020). Nonetheless, the wide δ^{138}Ba range of the solid load is quite surprising regarding the relative homogeneity of δ^{138}Ba in the rock forming the UCC and the weathering product of other large rivers (Nan *et al.*, 2018; Charbonnier *et al.*, 2020; Gou *et al.*, 2020).

3.2 Abundance and Isotope Signature of Ba in the Global Dissolved Riverine Export

The Ba abundance in the dissolved load varies from 0.05 µmol/L (Yenisey) to 0.76 µmol/L (HuangHe) and an average of 0.21 µmol/L (Table S-1), similar to the world average of 0.17 µmol/L estimated by Gaillardet *et al.* (2014).

However, Ba abundance in the dissolved load is likely influenced by water dilution. A way to cancel out this dilution effect is to normalise the Ba concentration to that a conservative element, here sodium (Na*), where "*" refers to the Cl-based correction from sea salt and halite inputs (Gaillardet *et al.*, 1997). Across our dataset, Ba/Na^* ratios also vary widely from 0.0001 (Irrawaddy) to 0.022 (Rio Negro).

The fraction of total Ba river transport that occurs as dissolved species can be calculated as follows:

$$w^X = \frac{[X]_{\text{diss}}}{[X]_{\text{diss}} + [X]_{\text{spm}} \times [\text{spm}]} \quad \text{Eq. S-2}$$

with $[X]_{\text{diss}}$ the dissolved concentration of X (*e.g.*, in µg/L), $[X]_{\text{spm}}$ the concentration of X in the river sediment (*e.g.*, in mg/kg) and [spm] the concentration of suspended sediment in the river (in g/L). In this study we use the long-term (typically multi-decadal) estimates of [spm] provided by (Milliman and Farnsworth, 2011).

The dissolved phase represents on average 20 % of total river Ba (*i.e.* $w^{Ba} \approx 0.2$; Fig. S-3, Table S-2). However, the global range of variation of w^{Ba} is very large: for some rivers, mainly those characterised by low erosion rates such as the Congo Basin, almost all Ba is transported in the dissolved load ($w^{Ba} \approx 0.86$), whereas in highly erosive contexts such as in the Huang He Basin, river Ba is entirely transported as solids ($w^{Ba} \approx 0.01$). The $\delta^{138}Ba$ values of the dissolved load of large rivers ($\delta^{138}Ba_{diss}$) range from −0.02 to +0.80 ‰ (Table S-1, Fig. S-2), on average significantly higher than that of the UCC (0.00 ± 0.04 ‰; Nan *et al.*, 2018). This first-order observation suggests that at the continental scale, the Ba dissolved flux to the ocean is influenced by processes such as secondary phase formation or biological uptake; by the release from rock types unaccounted for in estimates of the UCC composition; or by a combination thereof.

3.3 The Isotope Composition of the Global Ba Flux to the Ocean

According to the global Ba fluxes reported by Gaillardet *et al.* (2014) and Viers *et al.* (2009), our river sample set represents 44 % (340×10^3 t yr^{-1} of 860×10^3 t yr^{-1}) and 30 % (2387×10^3 t yr^{-1} of 7835×10^3 t yr^{-1}) of the river Ba

dissolved and solid fluxes to the ocean, respectively. These numbers indicate that our dataset is representative of the global riverine export of Ba.

Our estimates for the Ba isotope composition of the global dissolved Ba flux ($\delta^{138}Ba_{diss,global}$) and solid Ba flux ($\delta^{138}Ba_{spm,global}$) are 0.24 ± 0.02 ‰ and 0.07 ± 0.03 ‰, respectively. Note that these isotope signatures are representative of the global Ba river fluxes before they enter estuaries, and thus can be affected afterward by estuarine processes (Bridgestock *et al.*, 2021).

The $\delta^{138}Ba_{diss,global}$ calculated from our study is slightly higher than the previously reported figure (0.16 ‰; Cao *et al.*, 2020). The reason for the higher $\delta^{138}Ba_{diss,global}$ found here stems from the presence of rivers having higher $\delta^{138}Ba_{diss}$ in our dataset such as the Mackenzie, Congo and other Arctic rivers. Nonetheless, for those rivers where the comparison can be made, we note that our values are similar to those of Cao *et al.* (2020).

4. Derivation of Catchment-Scale Mass and Isotope Budget Equations

In the present study, we establish catchment-scale mass budgets for the two non-nutrient elements lithium (Li) and sodium (Na), for the major nutrient potassium (K) (Chaudhuri *et al.*, 2007) and for a nutrient-like trace element: barium (Ba) (Bullen and Chadwick, 2016; Charbonnier *et al.*, 2020).

The fate of a chemical element after its release by rock dissolution can be investigated using so-called "catchment-scale" or "river mass" budgets (Gaillardet *et al.*, 1995; Stallard, 1995). In this approach, we test whether for an element X the sum of the river fluxes of dissolved material derived from chemical weathering (F^X_{diss}) and of sediment derived from physical erosion (F^X_{sed}) reflects the input of rock material to the Earth surface (F^X_{rock}):

$$F^X_{rock} = F^X_{diss} + F^X_{sed} \qquad \text{Eq. S-3}$$

If Equation S-3 is valid for an element X, the catchment-scale mass budget of this element can be qualified as "balanced". Conversely, a mismatch between the two sides of Equation S-3 indicates either (1) a poor estimate of F^X_{rock}, (2) that the river export fluxes F^X_{diss} and F^X_{sed} have not been properly measured, or (3) that rivers do not

currently export the exact amount of X supplied to the Earth surface (in other words, that the catchment is currently accumulating or losing X), or any combination thereof. In terms of absolute fluxes, the term F^X_{rock} of Equation S-3 is usually estimated from the sum of F^X_{diss} and F^X_{sed}, which can be difficult to obtain except in relatively rare occasions where suitable river gauging protocols are in place. To circumvent this issue, we introduce soluble-to-insoluble element ratios. Noting first that for an insoluble element Y, $w^Y \approx 0$:

$$F^Y_{\text{rock}} = F^Y_{\text{sed}} \qquad \text{Eq. S-4}$$

Dividing Equation S-3 by Equation S-4, and recognizing that the flux ratio $\frac{F^X_i}{F^Y_i}$ is equal to the elemental abundance ratio $\left(\frac{X}{Y}\right)_i$:

$$\left(\frac{X}{Y}\right)_{\text{rock}} = \frac{F^X_{\text{diss}} + F^X_{\text{sed}}}{F^Y_{\text{sed}}} = \frac{F^X_{\text{sed}}}{F^Y_{\text{sed}}} + \frac{F^X_{\text{diss}}}{F^Y_{\text{sed}}} = \left(\frac{X}{Y}\right)_{\text{sed}} + \frac{F^X_{\text{diss}}}{F^Y_{\text{sed}}} \qquad \text{Eq. S-5}$$

The right-hand side of Equation S-5 still features flux terms that are difficult to measure directly. We divide each side of Equation S-5 by $\left(\frac{X}{Y}\right)_{\text{rock}}$ and use Equation S-4:

$$1 = \frac{(X/Y)_{\text{sed}}}{(X/Y)_{\text{rock}}} + \left(\frac{F^X_{\text{diss}}}{F^Y_{\text{sed}}}\right) / \left(\frac{F^X_{\text{rock}}}{F^Y_{\text{rock}}}\right) = \frac{\left(\frac{X}{Y}\right)_{\text{sed}}}{\left(\frac{X}{Y}\right)_{\text{rock}}} + \frac{F^X_{\text{diss}}}{F^X_{\text{rock}}} = (1 + \tau_x) + w^X \qquad \text{Eq. S-6}$$

where $1 + \tau_x$ is the ratio between $(X/Y)_{\text{sed}}$ and $(X/Y)_{\text{rock}}$, and represents the relative depletion of X in river sediment with respect to the source rock (using for notation purposes the definition of the so-called "mass transfer coefficient" τ_x classically used in weathering studies at the soil scale; *e.g.*, Brimhall *et al.*, 1991). The

$1+\tau_x$ term also corresponds to the inverse of the α-depletion factor of soluble elements ($\alpha^X = \frac{(X/Y)_{\text{rock}}}{(X/Y)_{\text{sed}}}$) in river sediments defined by Gaillardet *et al.* (1999a). The ratio $\frac{F^X_{\text{diss}}}{F^X_{\text{rock}}}$ represents the relative transport of X as a dissolved species, that is equal to w^X defined in Equation S-2.

By definition, Equation S-6 is valid when the riverine export balances the amount of material supplied to the critical zone through rock degradation. If not, the imbalance is quantified as follows:

$$f^X_{\text{imbalance}} = 1 - (1+\tau_x) - w^X = -\tau_x - w^X \qquad \text{Eq. S-7}$$

If $f^X_{\text{imbalance}} > 0$, X is "less exported" by rivers than predicted by rock degradation. Conversely, if $f^X_{\text{imbalance}} < 0$, X is "more exported" by rivers than predicted.

In the present study we apply this approach to the nutrient(-like) elements K and Ba. In principle this can also be done for the other major cations Ca and Mg. Nevertheless, the significant contribution of carbonate to F^X_{rock} as well as F^X_{diss}, and to a lesser extent F^X_{sed}, makes it difficult to constrain their catchment-scale mass budgets. All results of Equation S-6 are reported in Figure 2 as a cross-plot of $(1+\tau_X)$ *vs.* w^X.

Although the introduction of element ratios in lieu of flux ratios in Equation S-3 mitigates the issues associated with the estimation of absolute fluxes, considerable uncertainty might stem from the fact that different rock types have different $(X/Y)_{\text{rock}}$ ratios. The first reason why $(X/Y)_{\text{rock}}$ ratios might differ between rock types is the differences in magmatic compatibility, which translates into variability in $(X/Y)_{\text{rock}}$ ratios between different types of crystalline rocks. In that respect, for a given soluble element X the best choice for the insoluble element Y is an element with a magmatic compatibility similar to that of X. In this study, following the approach of Gaillardet *et al.* (1999a) we use the Ba/Th, K/Th, Li/Al, and Na/Sm ratios.

The second reason why $(X/Y)_{\text{rock}}$ might differ between rock types is the depletion of meta-sedimentary rocks in soluble elements X compared to their crystalline protoliths, due to the fact that such rocks have already undergone loss of soluble elements during previous weathering episodes (Gaillardet *et al.*, 1999a). However, we first

note that the Ba/Th ratio of igneous rocks and shales are relatively similar. Only andesites, which are significantly present in the Solimões, Stikine and Nass basins, show a much higher Ba/Th ratio (Charbonnier *et al.*, 2020). In this case, we compute the $(Ba/Th)_{rock}$ ratio as a mixture between andesites and shales rocks using the relative rock contribution estimated by Dellinger *et al.* (2017). Potassium shows a relatively limited range of variation (from 28,000 to 33,083 mg/kg; Taylor and McLennan, 1995; Rudnick and Gao, 2014) between igneous rocks and shales. Therefore, we assume a single $(K/Th)_{rock}$ value of 2,500 for all rock types. The variability in Na abundance between meta-sedimentary and crystalline rocks is the highest (Taylor and McLennan, 1995; Rudnick and Gao, 2014), due to the high solubility of Na during weathering and the absence of reverse weathering reactions in the ocean involving Na. When possible, we use independent constraints on the bedrock undergoing weathering for the Amazon and its tributaries, the Congo, the Changjiang, the Mackenzie, and the Ganges-Brahmaputra systems from Dellinger *et al.* (2017). For rivers for which we do not have the required data, we assumed that the river bed sediment chemistry is representative of that of bedrock, as coarse sediment are thought to best represent the products of erosion of the rock undergoing degradation, but with no measurable effect of chemical weathering (Potter, 1978; Dellinger *et al.*, 2014).

The comparison between the catchment-scale mass budgets of elements of importance for plant nutrition with those of elements with no physiological role is a test for the influence of biological cycling on global river solute export. Previous studies have already suggested that at the global scale the river mass budgets of Li is balanced (Dellinger *et al.*, 2015a, 2017). However, we re-visit these results in the scope of detecting any pattern specific to the rock-derived nutrients K and Ba. Below, we provide a comparison of river mass budget results of K, Na, and Li as a function of Ba.

The two bio-utilised elements Ba and K show negative imbalance (the difference between what is supplied to the critical zone by rock degradation and the riverine export; see Eqs. S-6 and S-7) for most of the studied rivers (Fig. S-4a), the cause for which is discussed in the main text. Here, we point out the interesting feature that Ba and K riverine imbalance show a positive relationship, suggesting a common mechanism for their missing components (see main text), whereas no correlation emerges between the imbalance of Ba and Na (Fig. S-4b). The Li imbalance is hardly resolvable given the uncertainties, suggesting a balanced mass budget (Fig. S-4c). We note that for a few rivers, a positive imbalance is observed: there, the export of rock-derived nutrients outpaces

their supply to the Earth surface by the rock degradation. This is the case for the St. Lawrence River, where relatively recent ice cap retreat might result in an imbalance in the dissolved and solid riverine export (Gaillardet *et al.*, 1999a). In tropical rivers showing this type of positive imbalance, such as the Congo and Negro rivers, the presence of organic colloids enhanced the transport as a dissolved species of insoluble elements such as Th, thus compromising the use of Equation S-6 (Charbonnier *et al.*, 2020). In cold Arctic rivers such as the Fraser and the Mackenzie, source rocks may contain unaccounted-for rock sources of Ba—thought to be linked to the presence of black shale rocks in the catchment—that contribute to the riverine export (Guay and Falkner, 1998; Charbonnier *et al.*, 2022).

The same type of mass balance can be performed using isotope ratios (see Bouchez *et al.*, 2013). In such approach, the flux-weighted sum of the solid and dissolved isotope compositions should in principle be equal to the isotope composition of the rock undergoing weathering:

$$\delta^{X}_{\mathrm{rock}} = w^{X} \times \delta^{X}_{\mathrm{diss}} + (1 - w^{X}) \times \delta^{X}_{\mathrm{sed}} \qquad \text{Eq. S-8}$$

with $\delta^{X}_{\mathrm{rock}}$, $\delta^{X}_{\mathrm{diss}}$, and $\delta^{X}_{\mathrm{sed}}$ the isotope composition of element *X* in the rock undergoing weathering, the river dissolved load, and the river solid load, respectively. As for elemental mass balance, any difference between the value of $\delta^{X}_{\mathrm{rock}}$ calculated from river loads (right-hand side of Eq. S-8) and that estimated for bedrock from independent constraints (left-hand side of Eq. S-8) suggests that a fractionated reservoir of *X* is not exported by river, or at least not sampled properly in the river export.

Here, this calculation is performed for Ba and Li based on our own Ba data and Li data from Dellinger *et al.*, (2014, 2015b, 2017) and Wang *et al.* (2015) (see Table S-2). We took the estimation of the continental crust of Ba from Nan *et al.* (2018) for $\delta^{\mathrm{Ba}}{}_{\mathrm{rock}}$ since there is, on average, no significant variation between different rock types. $\delta^{\mathrm{Li}}{}_{\mathrm{rock}}$ are taken from (Dellinger *et al.*, 2017), as the isotope composition of bedrock Li can vary widely between catchments, due to the difference in Li isotope composition between igneous and sedimentary silicate rocks (Dellinger *et al.*, 2015a). Results are reported in Table S-2 and discussed in the main text.

5. Testing for a "Poorly Gauged Flux" as an Explanation of the Observed Imbalance in Rock-Derived Nutrients in River Exports

Here we test the hypothesis that part of the observed rock-derived nutrients imbalance is due to a "poorly gauged flux", as river export of coarse vegetation debris, in particular during high-flow events, is likely to be missed by classically-used sampling schemes of large rivers (see section S-1 above) (Abbe and Montgomery, 2003; Heartsill Scalley *et al.*, 2012; Wohl *et al.*, 2012; Uhlig *et al.*, 2017). To that effect, we first quantify the flux of river particulate organic carbon required to account for the observed riverine K imbalance (F^{C}_{miss}) following Charbonnier *et al.* (2020):

$$F^{C}_{miss} = \frac{F^{K}_{miss}}{(K/C)_{bio}} \quad \text{Eq. S-9}$$

with $(K/C)_{bio}$ the K/C ratio of the biological component exported by rivers (data from Charbonnier *et al.*, 2020); F^{C}_{miss} the required missing carbon flux, and F^{K}_{miss} the estimated missing potassium flux calculated as follows:

$$F^{K}_{miss} = D \times [K]_{rock} \times f^{K}_{imbalance} \quad \text{Eq. S-10}$$

with D the denudation rate D is the sum of the chemical weathering and physical erosion rates, typically estimated at the catchment-scale using either the river fluxes of weathering-derived solutes and sediments; or using the concentration of the cosmogenic nuclide beryllium-10 in river sands. Here it is used as a proxy for the rate at which rock is delivered to the Critical Zone at the catchment scale.

In Fig S-5, we compare the inferred carbon missing flux from Equation S-9 with independent constraints on particulate carbon riverine export (Galy *et al.*, 2015). This comparison is made using the relationships between POC export and the denudation rate D as (1) estimated from our own data on rock-derived nutrient (Eq. S-9) and (2) reported by Galy *et al.* (2015) from actual measurements of POC export. The relationship estimated from our data is two orders of magnitude higher than the observed relationship (Fig. S-5). This difference is likely too large to be realistic, suggesting that a poorly gauged POC flux alone is not responsible for the observed imbalance in rock-

derived nutrients catchment-scale mass budget.

Alternatively, tree logging by human activity could be responsible for such a poorly gauged flux. Nonetheless, river catchments characterised by the strongest negative imbalance in the river mass budgets rock-derived nutrients (Orinoco, Niger, Ganges-Brahmaputra) do not correspond to regions where deforestation is the most intense (Canada, Northern, Russia, Amazon plains and Congo Basin; Curtis *et al.*, 2018). Second, using the Global Forest Change map (Hansen *et al.*, 2013; https://glad.earthengine.app/view/global-forest-change), we quantified the relative forest lost from 2000 to 2020 for five basins: Amazon, Congo, Orinoco, Fraser, and Mackenzie. These basins feature different degrees of deforestation as well as different degrees of K depletion in rivers. The comparison between these two parameters does not show any meaningful relationship (see Fig. S-6). This first-order examination suggests that logging cannot account for the deleted K component of large river rivers.

A Limited Role of Anthropogenic Inputs to the K Riverine Budget

Regarding the potential role of fertiliser on the global K riverine budget, we first note that most of rivers show a depletion in K export, whereas any additional, non-accounted for source (such as fertiliser or atmospheric inputs) should lead to an excess of K in rivers. In addition, following the approach of Li *et al.* (2022), we compare the average NO_3/Na* and NO_3/K ratios for our rivers of 0.45 and 0.89, respectively, which are much lower than the anthropogenic signatures of fertilisers at NO_3/Na = 7 and NO_3/K = 4 (Chetelat *et al.*, 2008). In fact, across our dataset only the Changjiang shows a relatively high NO_3/K ratio of around 3. Of course, these elemental ratios only disclose the contribution of K-fertiliser to the dissolved load. However, given the high solubility of K-fertiliser (Mikkelsen, 2007), the latter should have a minor influence on the K river solid flux, that represents the main path of K riverine export. For these reasons, we assume that fertiliser should play a minor role in the K mass budget of large rivers.

6. Testing for a "Growing Organic Pool" as an Explanation of the Observed Imbalance in Rock-Derived Nutrients in River Exports

In this study, we explore the possibility that biological uptake is responsible for the observed widespread imbalance

in the riverine export of nutrient-like elements. One possible explanation might lie in short-term variability in the biota size at the catchment scale, which leads to net nutrient uptake or release. In particular, changes in the magnitude of the land carbon sink over the last decades (Pan *et al.*, 2011) might lead to imbalance in catchment-scale rock-derived nutrient export. As a test of this hypothesis, below we provide a derivation for quantifying the amount of the rock-derived nutrient that is taken up for a given increase in the size of the continental biota (in terms of total biomass), relative to the supply of this nutrient by rock degradation. We define the rate of increase of the size of the biota as:

$$r = \frac{d(M_{\mathrm{bio}})}{dt} \qquad \text{Eq. S-11}$$

where M_{bio} is the mass of the biota reservoir within a given large river catchment. Such an increase of the biota size is accompanied by an incremental flux of uptake of the nutrient X:

$$U^X = r \times [X]_{\mathrm{bio}} \qquad \text{Eq. S-12}$$

with $[\mathrm{X}]_{\mathrm{bio}}$ the concentration of X in the biota.

Then, normalizing U^X by the amount of X supplied by rock degradation yields the uptake of the nutrient X by the biota relative to the supply of X provided by rock degradation, a ratio hereafter called β:

$$\beta = \frac{r \times [X]_{\mathrm{bio}}}{D \times [X]_{\mathrm{rock}}} = \frac{F^X_{\mathrm{bio}}}{F^X_{\mathrm{rock}}} \qquad \text{Eq. S-13}$$

The β value is basically an estimate of the catchment-scale imbalance of X (as defined in Eq. S-7 above) that should be observed if the biomass in the catchment were increasing at a rate r, given a catchment-scale denudation D. Thus, calculated values for a given r can then be compared to observed estimates of X imbalance to assess the plausibility of the "growing organic pool" scenario. We calculate β for an incremental increase in the biota size of 0.1 and 0.2 % as estimated recently for the average yearly land C sink on the continents (Friedlingstein *et al.*, 2020), for a range of D of 10–500 t/km^2/yr as observed in most large river catchments (Milliman and Farnsworth, 2011; Wittmann *et al.*,

2020) for a range of elements (Al, B, Ba, Ca, Cu, Fe, Mg, Mn, Mo, Ni, P, K, Rb, Na, Sr, Zn) with different abundances in plants, ranging from essential nutrients to non-nutrient elements (Table S-3). We calculate $[K]_{bio}$ values using (a) a compilation for the chemical composition of plant parts from Charbonnier *et al.* (2020) and (b) a compilation for the chemical composition of leaves made in the frame of the present study. We plot the β value for K in Fig. S-7 as the latter is a major rock-derived nutrient for which we observed a riverine imbalance (Fig. 2). The order-of-magnitude difference between the two panels of Fig. S-7 is driven by the difference in the value of $[K]_{bio}$ used, showing how this calculation is sensitive to this poorly constrained parameter.

With this simple model, explaining the observed range K riverine imbalance (Fig. S-7) requires that $[K]_{bio}$ is higher than that proposed by Charbonnier *et al.* (2020). This is plausible as the compilation of Charbonnier *et al.* (2020) might be biased by an important number data entries of trunk samples, being characterised by lower concentrations of rock-derived nutrients compared to other plant tissues such as foliage. Conversely, the β value of K calculated with the foliage compilation should lead to an overestimation of the $[K]_{bio}$, thereby providing a "maximum" estimate. Therefore, although this calculation is subject to large uncertainties, it provides 1) a range of minimum and maximum uptake of K as a function of estimates for catchment-scale biomass growth denudation and 2) a first estimate for β values (as $[X]_{bio}$ remains hard to constrain) on major and trace elements at the Earth surface (see Tables S-3). This analysis shows that, except for elements such as Al or Na, biological cycling could in principle affects most of the elements and their isotope signatures exported by rivers. However, this requires a long-term growing organic pool to influence riverine export, of a magnitude that seems unlikely at the global scale (see main text).

Supplementary Tables

Table S-1 Elemental and isotope data on large rivers.

Table S-2 Results of the river mass budget calculations (Supplementary Information section 4).

Table S-3 Compilation of abundance of rock-derived nutrients in plants used to test for the "growing organic pool " scenario (Supplementary Information section 6).

Tables S-1 to S-3 are available for download (Excel) from the online version of the article at https://doi.org/10.7185/geochemlet.2214.

Supplementary Figures

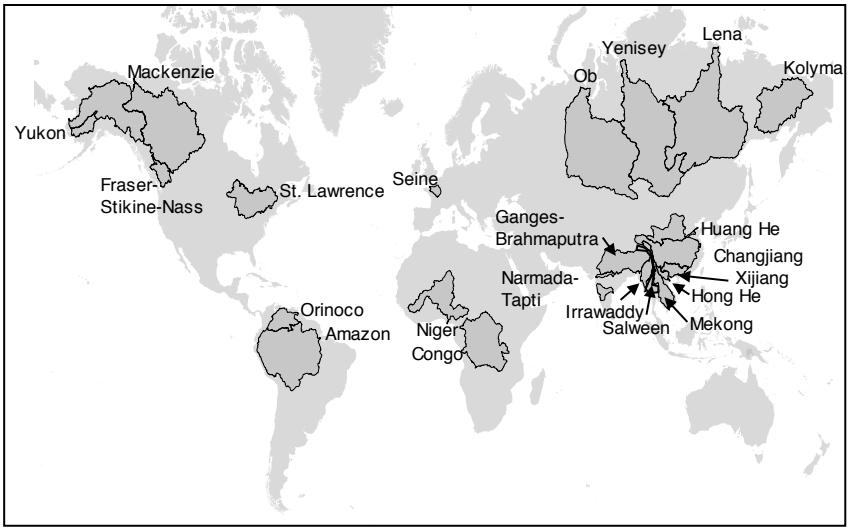

Figure S-1 World map showing the sample locations and river basins.

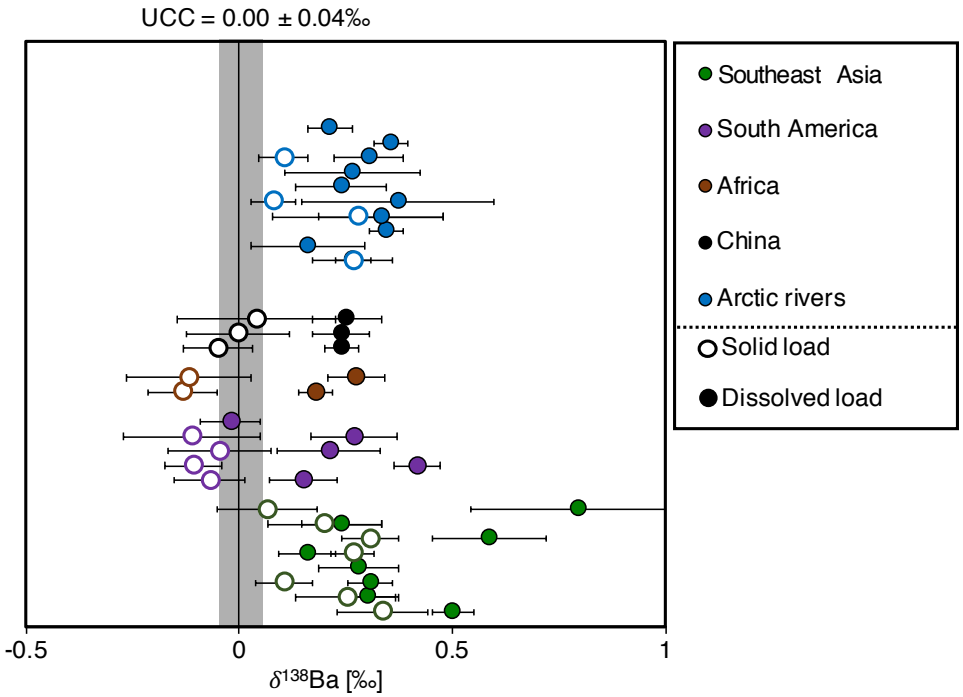

Figure S-2 Ba isotope composition of the dissolved and solid loads of the world's largest rivers. The value of the Upper Continental Crust (UCC), taken as the composition of the source rock, is derived from Nan *et al.* (2018).

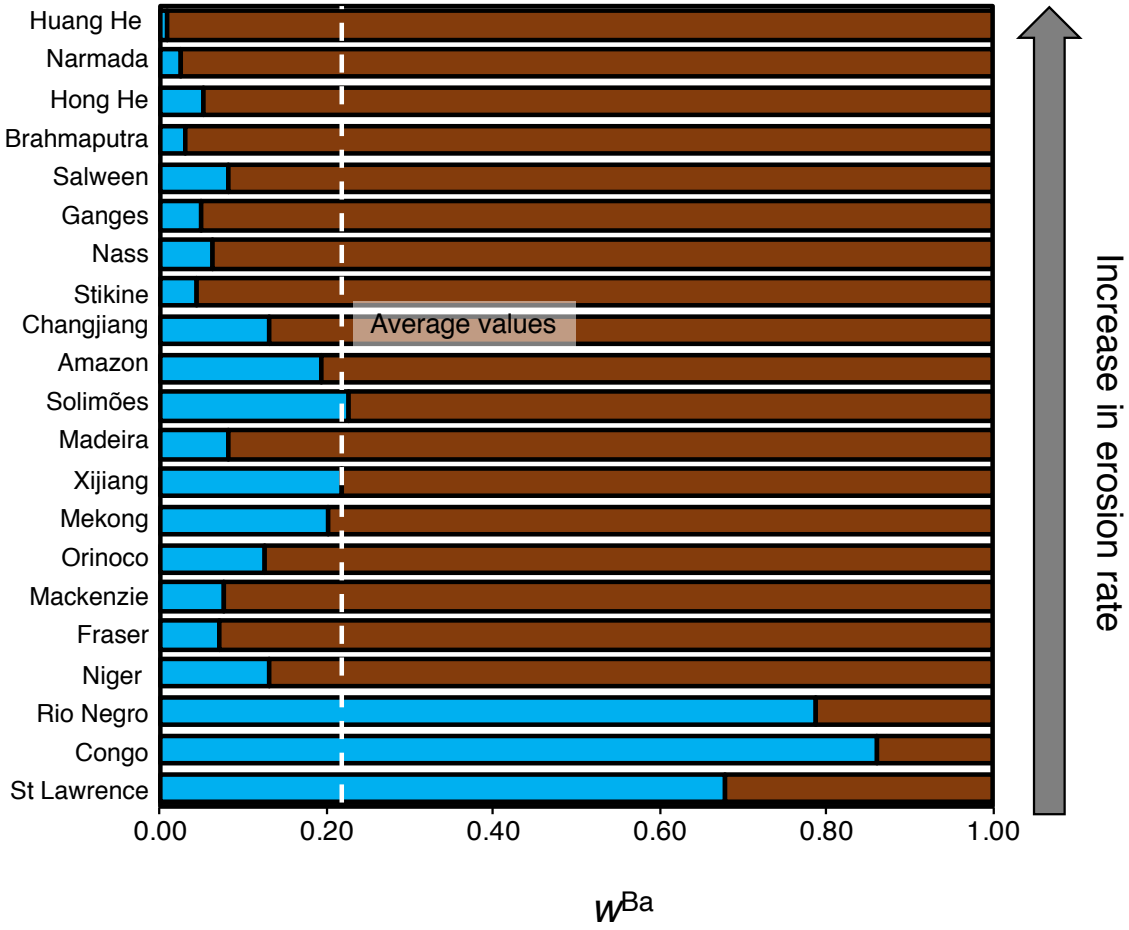

Figure S-3 Partitioning of Ba (w^{Ba}) between the river dissolved (blue) and the solid loads (brown) across the world largest rivers.

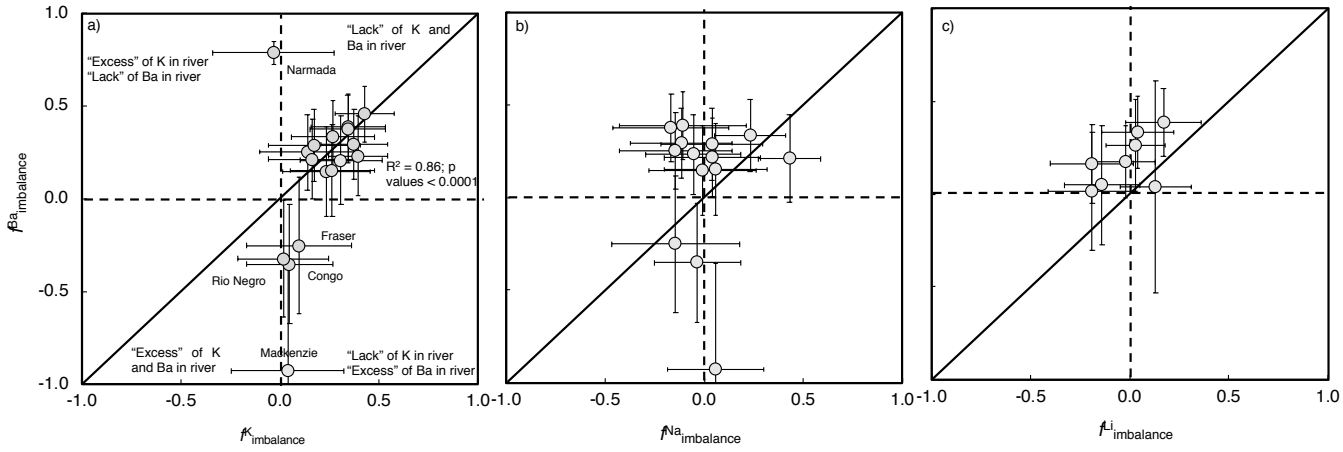

Figure S-4 Comparison of the Ba imbalance with **(a)** K imbalance, **(b)** Na imbalance, and **(c)** Li imbalance in their river mass budgets, as calculated using Equation S-7.

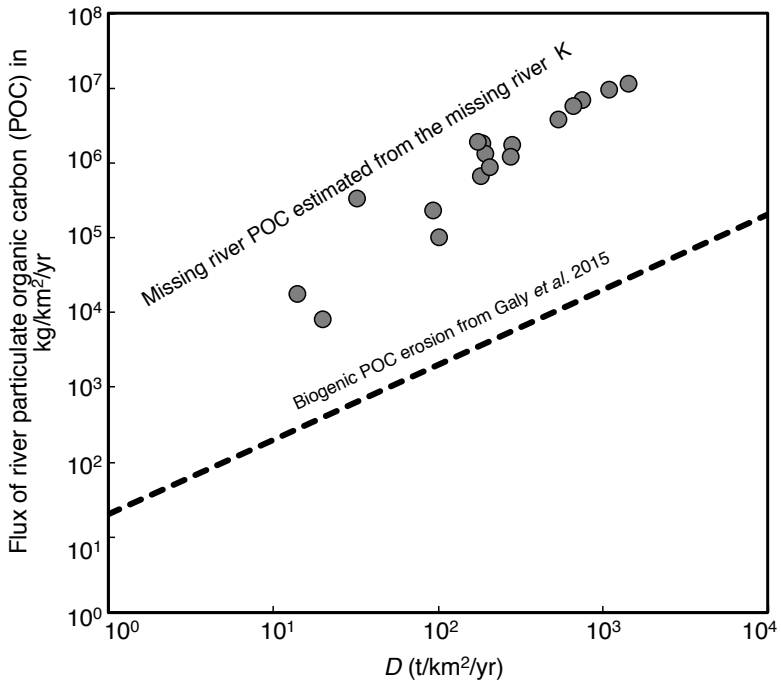

Figure S-5 Comparison of the relationship between denudation rate (D) and river particulate organic carbon (POC) flux estimated by Galy *et al.* (2015) from actual measurements of POC (black stippled line), and the same relationship calculated from catchment-scale mass budgets of rock-derived nutrients (Eq. S-9) shown as data points.

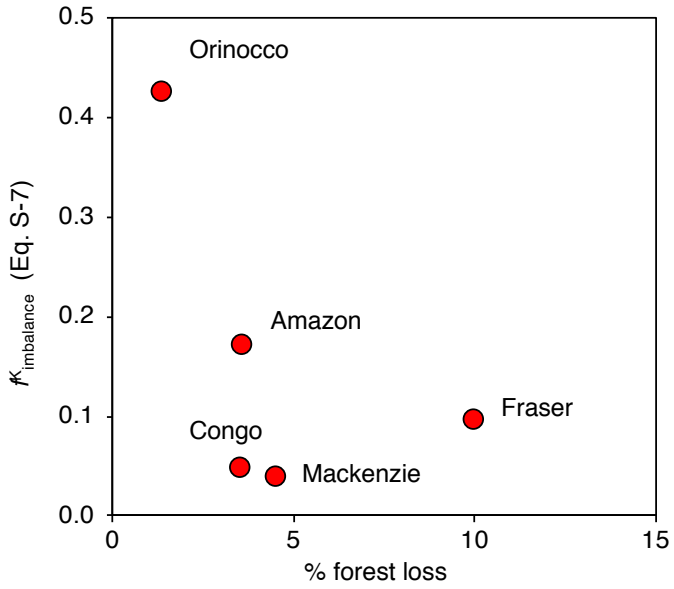

Figure S-6 Comparison between the relative K imbalance (quantified using Eq. S-7) and the relative forest loss during the last twenty years (2000–2020) using the Global Forest Change map (Hansen *et al.*, 2013; see Section 5).

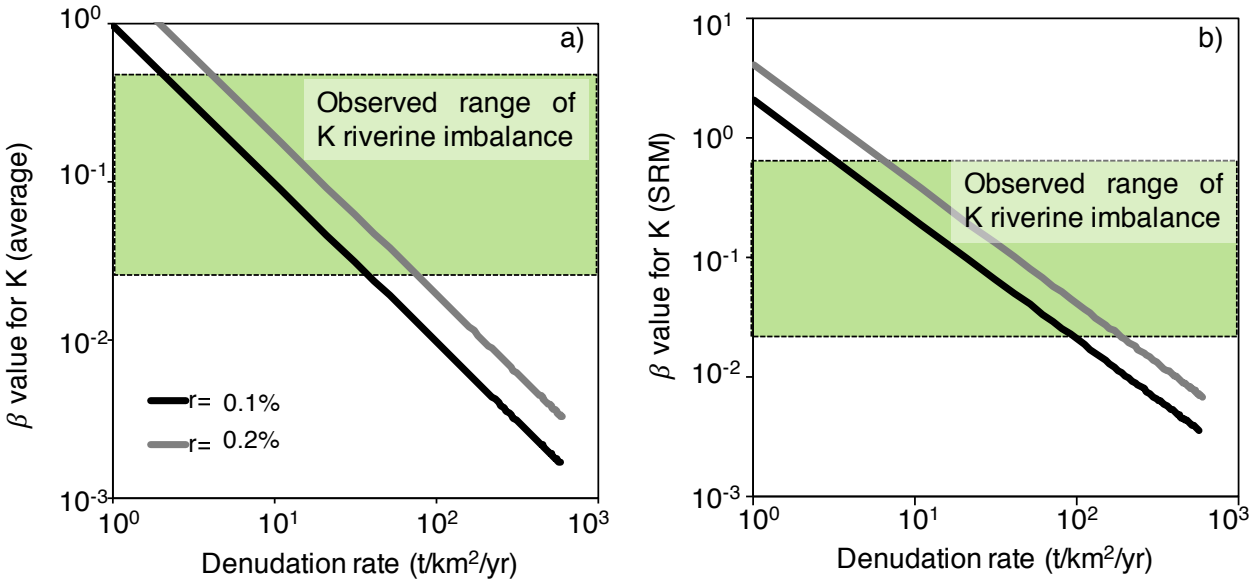

Figure S-7 β value (expected catchment-scale imbalance of a rock-derived nutrient in the case of biomass growth; Eq. S-13) of K for a denudation ranging from 10 to 500 t/km^2/yr. The green band indicates the range of K imbalance in the catchment-scale mass budgets of large rivers, as computed from Equation S-7. In the legend, r corresponds to the yearly relative rate of biomass growth. Results presented in **(a)** correspond to those obtained using a K content in organic matter ($[K]_{bio}$) taken from the compilation of Charbonnier *et al*. (2020) and those in **(b)** rely on the use of the chemical composition of leaf reference materials.

Supplementary Information References

Abbe, T.B., Montgomery, D.R. (2003) Patterns and processes of wood debris accumulation in the Queets river basin, Washington. *Geomorphology* 51, 81–107. https://doi.org/10.1016/S0169-555X(02)00326-4

Bouchez, J., Gaillardet, J., France-Lanord, C., Maurice, L., Dutra-Maia, P. (2011) Grain size control of river suspended sediment geochemistry: Clues from Amazon River depth profiles. *Geochemistry, Geophysics, Geosystems* 12, Q03008. https://doi.org/10.1029/2010GC003380

Bouchez, J., von Blanckenburg, F., Schuessler, J.A. (2013) Modeling novel stable isotope ratios in the weathering zone. *American Journal of Science* 313, 267–308. https://doi.org/10.2475/04.2013.01

Bridgestock, L., Hsieh, Y.-T., Porcelli, D., Homoky, W.B., Bryan, A., Henderson, G.M. (2018) Controls on the barium isotope compositions of marine sediments. *Earth and Planetary Science Letters* 481, 101–110. https://doi.org/10.1016/j.epsl.2017.10.019

Bridgestock, L., Hsieh, Y.-T., Porcelli, D., Henderson, G.M. (2019) Increased export production during recovery from the Paleocene–Eocene thermal maximum constrained by sedimentary Ba isotopes. *Earth and Planetary Science Letters* 510, 53–63. https://doi.org/10.1016/j.epsl.2018.12.036

Bridgestock, L., Nathan, J., Paver, R., Hsieh, Y.-T., Porcelli, D., Tanzil, J., Holdship, P., Carrasco, G., Annammala, K.V., Swarzenski, P.W., Henderson, G.M. (2021) Estuarine processes modify the isotope composition of dissolved riverine barium fluxes to the ocean. *Chemical Geology* 579, 120340. https://doi.org/10.1016/j.chemgeo.2021.120340

Brimhall, G.H., Lewis, C.J., Ford, C., Bratt, J., Taylor, G., Warin, O. (1991) Quantitative geochemical approach to pedogenesis: importance of parent material reduction, volumetric expansion, and eolian influx in lateritization. *Geoderma* 51, 51–91. https://doi.org/10.1016/0016-7061(91)90066-3

Bullen, T., Chadwick, O. (2016) Ca, Sr and Ba stable isotopes reveal the fate of soil nutrients along a tropical climosequence in Hawaii. *Chemical Geology* 422, 25–45. https://doi.org/10.1016/j.chemgeo.2015.12.008

Cao, Z., Siebert, C., Hathorne, E.C., Dai, M., Frank, M. (2020) Corrigendum to "Constraining the oceanic barium cycle with stable barium isotopes" [Earth Planet. Sci. Lett. 434 (2016) 1–9]. *Earth and Planetary Science Letters* 530, 116003. https://doi.org/10.1016/j.epsl.2019.116003

Charbonnier, Q., Moynier, F., Bouchez, J. (2018) Barium isotope cosmochemistry and geochemistry. *Science Bulletin* 63, 385–394. https://doi.org/10.1016/j.scib.2018.01.018

Charbonnier, Q., Bouchez, J., Gaillardet, J., Gayer, É. (2020) Barium stable isotopes as a fingerprint of biological cycling in the Amazon River basin. *Biogeosciences* 17, 5989–6015. https://doi.org/10.5194/bg-17-5989-2020

Charbonnier, Q., Bouchez, J., Gaillardet, J., Calmels, D., Dellinger, M. (2022) The influence of black shale weathering on riverine barium isotopes. *Chemical Geology* 594, 120741. https://doi.org/10.1016/j.chemgeo.2022.120741

Chaudhuri, S., Clauer, N., Semhi, K. (2007) Plant decay as a major control of river dissolved potassium: A first estimate. *Chemical Geology* 243, 178–190. https://doi.org/10.1016/j.chemgeo.2007.05.023

Chetelat, B., Liu, C.Q., Zhao, Z.Q., Wang, Q.L., Li, S.L., Li, J., Wang, B.L. (2008) Geochemistry of the dissolved load of the Changjiang Basin rivers: Anthropogenic impacts and chemical weathering. *Geochimica et Cosmochimica Acta* 72, 4254–4277. https://doi.org/10.1016/j.gca.2008.06.013

Curtis, P.G., Slay, C.M., Harris, N.L., Tyukavina, A., Hansen, M.C. (2018) Classifying drivers of global forest loss. *Science* 361, 1108–1111. https://doi.org/10.1126/science.aau3445

Dellinger, M., Gaillardet, J., Bouchez, J., Calmels, D., Galy, V., Hilton, R.G., Louvat, P., France-Lanord, C. (2014) Lithium isotopes in large rivers reveal the cannibalistic nature of modern continental weathering and erosion. *Earth and Planetary Science Letters* 401, 359–372. https://doi.org/10.1016/j.epsl.2014.05.061

Dellinger, M., Bouchez, J., Gaillardet, J., Faure, L. (2015a) Testing the Steady State Assumption for the Earth's Surface Denudation Using Li Isotopes in the Amazon Basin. *Procedia Earth and Planetary Science* 13, 162–168. https://doi.org/10.1016/j.proeps.2015.07.038

Dellinger, M., Gaillardet, J., Bouchez, J., Calmels, D., Louvat, P., Dosseto, A., Gorge, C., Alanoca, L., Maurice, L. (2015b) Riverine Li isotope fractionation in the Amazon River basin controlled by the weathering regimes. *Geochimica et Cosmochimica Acta* 164, 71–93. https://doi.org/10.1016/j.gca.2015.04.042

Dellinger, M., Bouchez, J., Gaillardet, J., Faure, L., Moureau, J. (2017) Tracing weathering regimes using the lithium isotope composition of detrital sediments. *Geology* 45, 411–414. https://doi.org/10.1130/G38671.1

Friedlingstein, P., O'Sullivan, M., Jones, M.W., Andrew, R.M., Hauck, J., *et al.* (2020) Global Carbon Budget 2020. *Earth System Science Data* 12, 3269–3340. https://doi.org/10.5194/essd-12-3269-2020

Gaillardet, J., Dupré, B., Allègre, C.J. (1995) A global geochemical mass budget applied to the Congo Basin rivers: erosion rates and continental crust composition. *Geochimica et Cosmochimica Acta* 59, 3469–3485. https://doi.org/10.1016/0016-7037(95)00230-W

Gaillardet, J., Dupre, B., Allegre, C.J., Négrel, P. (1997) Chemical and physical denudation in the Amazon River Basin. *Chemical Geology* 142, 141–173. https://doi.org/10.1016/S0009-2541(97)00074-0

Gaillardet, J., Dupré, B., Allègre, C.J. (1999a) Geochemistry of large river suspended sediments: silicate weathering or recycling tracer? *Geochimica et Cosmochimica Acta* 63, 4037–4051. https://doi.org/10.1016/S0016-7037(99)00307-5

Gaillardet, J., Dupré, B., Louvat, P., Allègre, C.J. (1999b) Global silicate weathering and CO_2 consumption rates deduced from the chemistry of large rivers. *Chemical Geology* 159, 3–30. https://doi.org/10.1016/S0009-2541(99)00031-5

Gaillardet, J., Viers, J., Dupré, B. (2014) 7.7 - Trace Elements in River Waters. In: Holland, H.D., Turekian, K.K. (Eds.) *Treatise on Geochemistry*. Second Edition, Elsevier, Amsterdam, 195–235. https://doi.org/10.1016/B978-0-08-095975-7.00507-6

Galy, V., France-Lanord, C., Lartiges, B. (2008) Loading and fate of particulate organic carbon from the Himalaya to the Ganga-Brahmaputra delta. *Geochimica et Cosmochimica Acta* 72, 1767–1787. https://doi.org/10.1016/j.gca.2008.01.027

Galy, V., Peucker-Ehrenbrink, B., Eglinton, T. (2015) Global carbon export from the terrestrial biosphere controlled by erosion. *Nature* 521, 204–207. https://doi.org/10.1038/nature14400

Garçon, M., Chauvel, C., France-Lanord, C., Limonta, M., Garzanti, E. (2014) Which minerals control the Nd–Hf–Sr–Pb isotopic compositions of river sediments? *Chemical Geology* 364, 42–55. https://doi.org/10.1016/j.chemgeo.2013.11.018

Gou, L.F. *et al.* (2020) Seasonal riverine barium isotopic variation in the middle Yellow River: Sources and fractionation. *Earth and Planetary Science Letters* 531, 115990. https://doi.org/10.1016/j.epsl.2019.115990

Guay, C.K., Falkner, K.K. (1998) A survey of dissolved barium in the estuaries of major Arctic rivers and adjacent seas. *Continental Shelf Research* 18, 859–882. https://doi.org/10.1016/S0278-4343(98)00023-5

Hansen, M.C. *et al.* (2013) High-Resolution Global Maps of 21st-Century Forest Cover Change. *Science* 342, 850–853. https://doi.org/10.1126/science.1244693. Data available on-line from: http://earthenginepartners.appspot.com/science-2013-global-forest.

Heartsill Scalley, T., Scatena, F.N., Moya, S., Lugo, A.E. (2012) Long-term dynamics of organic matter and elements exported as coarse particulates from two Caribbean montane watersheds. *Journal of Tropical Ecology* 28, 127–139. https://doi.org/10.1017/S0266467411000733

Henchiri, S., Gaillardet, J., Dellinger, M., Bouchez, J., Spencer, R.G.M. (2016) Riverine dissolved lithium isotopic signatures in low-relief central Africa and their link to weathering regimes. *Geophysical Research Letters* 43, 4391–4399. https://doi.org/10.1002/2016GL067711

Holmes, R.M. *et al.* (2012) Seasonal and Annual Fluxes of Nutrients and Organic Matter from Large Rivers to the Arctic Ocean and Surrounding Seas. *Estuaries and Coasts* 35, 369–382. https://doi.org/10.1007/s12237-011-9386-6

Horner, T.J., Kinsley, C.W., Nielsen, S.G. (2015) Barium-isotopic fractionation in seawater mediated by barite cycling and oceanic circulation. *Earth and Planetary Science Letters* 430, 511–522. https://doi.org/10.1016/j.epsl.2015.07.027

Lemarchand, D., Gaillardet, J., Lewin, E., Allegre, C.J. (2000) The influence of rivers on marine boron isotopes and implications for reconstructing past ocean pH. *Nature* 408, 951–954. https://doi.org/10.1038/35050058

Li, X., Han, G., Liu, M., Liu, J., Zhang, Q., Qu, R. (2022) Potassium and its isotope behaviour during chemical weathering in a tropical catchment affected by evaporite dissolution. *Geochimica et Cosmochimica Acta* 316, 105–121. https://doi.org/10.1016/j.gca.2021.10.009

Mikkelsen, R.L. (2007) Managing potassium for organic crop production. *HortTechnology* 17, 455–460. https://doi.org/10.21273/HORTTECH.17.4.455

Milliman, J.D., Farnsworth, K.L. (2011) *River Discharge to the Coastal Ocean: A Global Synthesis*. First Edition, Cambridge University Press, Cambridge. https://doi.org/10.1017/CBO9780511781247

Miyazaki, T., Kimura, J.-I., Chang, Q. (2014) Analysis of stable isotope ratios of Ba by double-spike standard-sample bracketing using multiple-collector inductively coupled plasma mass spectrometry. *Journal of Analytical Atomic Spectrometry* 29, 483–490. https://doi.org/10.1039/c3ja50311a

Nan, X.-Y., Yu, H.-M., Rudnick, R.L., Gaschnig, R.M., Xu, J., Li, W.-Y., Zhang, Q., Jin, Z.-D., Li, X.-H., Huang, F. (2018) Barium isotopic composition of the upper continental crust. *Geochimica et Cosmochimica Acta* 233, 33–49. https://doi.org/10.1016/j.gca.2018.05.004

Pan, Y. *et al.* (2011) A Large and Persistent Carbon Sink in the World's Forests. *Science* 333, 988–993. https://doi.org/10.1126/science.1201609

Potter, P.E. (1978) Petrology and Chemistry of Modern Big River Sands. *The Journal of Geology* 86, 423–449. https://doi.org/10.1086/649711

Rudnick, R.L., Gao, S. (2014) 4.1 - Composition of the Continental Crust. In: Holland, H.D., Turekian, K.K. (Eds.) *Treatise on Geochemistry*. Second Edition, Elsevier, Amsterdam, 1–51. https://doi.org/10.1016/B978-0-08-095975-7.00301-6

Spencer, R.G.M. *et al*. (2012) An initial investigation into the organic matter biogeochemistry of the Congo River. *Geochimica et Cosmochimica Acta* 84, 614–627. https://doi.org/10.1016/j.gca.2012.01.013

Stallard, R.F. (1995) Tectonic, Environmental, and Human Aspects of Weathering and Erosion: A Global Review using a Steady-State Perspective. *Annual Review of Earth and Planetary Sciences* 23, 11–39. https://doi.org/10.1146/annurev.ea.23.050195.000303

Taylor, S.R., McLennan, S.M. (1995) The geochemical evolution of the continental crust. *Reviews of Geophysics* 33, 241–265. https://doi.org/10.1029/95RG00262

Tipper, E.T., Galy, A., Gaillardet, J., Bickle, M.J., Elderfield, H., Carder, E.A. (2006) The magnesium isotope budget of the modern ocean: Constraints from riverine magnesium isotope ratios. *Earth and Planetary Science Letters* 250, 241–253. https://doi.org/10.1016/j.epsl.2006.07.037

Tipper, E.T., Gaillardet, J., Galy, A., Louvat, P., Bickle, M.J., Capmas, F. (2010) Calcium isotope ratios in the world's largest rivers: A constraint on the maximum imbalance of oceanic calcium fluxes. *Global Biogeochemical Cycles* 24, GB3019. https://doi.org/10.1029/2009GB003574

Uhlig, D., Schuessler, J.A., Bouchez, J., Dixon, J.L., von Blanckenburg, F. (2017) Quantifying nutrient uptake as driver of rock weathering in forest ecosystems by magnesium stable isotopes. *Biogeosciences* 14, 3111–3128. https://doi.org/10.5194/bg-14-3111-2017

van Zuilen, K., Nägler, T.F., Bullen, T.D. (2016) Barium Isotopic Compositions of Geological Reference Materials. *Geostandards and Geoanalytical Research* 40, 543–558. https://doi.org/10.1111/ggr.12122

Viers, J., Dupré, B., Gaillardet, J. (2009) Chemical composition of suspended sediments in World Rivers: New insights from a new database. *Science of The Total Environment* 407, 853–868. https://doi.org/10.1016/j.scitotenv.2008.09.053

Wang, Q.L., Chetelat, B., Zhao, Z.Q., Ding, H., Li, S.L., Wang, B.L., Li, J., Liu, X.L. (2015) Behavior of lithium isotopes in the Changjiang River system: Sources effects and response to weathering and erosion. *Geochimica et Cosmochimica Acta* 151, 117–132. https://doi.org/10.1016/j.gca.2014.12.015

Wittmann, H., Oelze, M., Gaillardet, J., Garzanti, E., von Blanckenburg, F. (2020) A global rate of denudation from cosmogenic nuclides in the Earth's largest rivers. *Earth-Science Reviews* 204, 103147. https://doi.org/10.1016/j.earscirev.2020.103147

Wohl, E., Dwire, K., Sutfin, N., Polvi, L., Bazan, R. (2012) Mechanisms of carbon storage in mountainous headwater rivers. *Nature Communications* 3, 1263. https://doi.org/10.1038/ncomms2274